

Cite this: *Nanoscale*, 2011, **3**, 1171

www.rsc.org/nanoscale

PAPER

## Nanoscale electrical probing of heterogeneous ceramics: the case of giant permittivity calcium copper titanate ( $\text{CaCu}_3\text{Ti}_4\text{O}_{12}$ )

Patrick Fiorenza,<sup>a</sup> Vito Raineri,<sup>a</sup> Matthew C. Ferrarelli,<sup>b</sup> Derek C. Sinclair<sup>b</sup> and Raffaella Lo Nigro<sup>\*a</sup>

Received 4th November 2010, Accepted 1st December 2010

DOI: 10.1039/c0nr00828a

Scanning Probe Microscopy with conductive tips has been used to image and study the dielectric properties of giant permittivity  $\text{CaCu}_3\text{Ti}_4\text{O}_{12}$  ceramics at the nanoscale. Since measurements are generally carried out on sections of a sample, particular attention has been devoted to possible artefacts due to surface imperfections, such as substantial surface roughness and/or contamination that can result in controversial interpretation, particularly at nanometric spatial dimensions. A reliable surface investigation has been carried out after the definition of both the physical and geometrical unbiased criteria to avoid any artefacts due to surface roughness and/or anomalous tip-sample contact variations. The presence of insulating grain boundaries and the measurement of a depletion layer at the grain-grain boundary interfaces unambiguously demonstrate the relevance of the Internal Barrier Layer Capacitor effect, among all the proposed physical mechanisms, to explain the giant dielectric behaviour. Such imaging provided a clear correlation between the macroscopic dielectric properties and the nanometric structure at the interfaces. Moreover, the “general criteria” for reliable nanoelectrical characterization as well as the related measurement resolution have been defined.

### Introduction

Dielectrics are often electrically heterogeneous materials and many among them are complex oxides.<sup>1</sup> In this context, calcium copper titanate,  $\text{CaCu}_3\text{Ti}_4\text{O}_{12}$  (CCTO), represents the most recently debated oxide because of the controversial definition of the origin of its giant permittivity ( $10^4$ – $10^5$  in the  $10^1$ – $10^6$  Hz range), which remains constant from 100 to 600 K, while it rapidly drops to 100 below 100 K.<sup>2–12</sup> In particular, several macroscopic and also some microscopic scale investigations pointed out the possibility to explain the giant permittivity ( $k$ ) of CCTO ceramics in terms of an Internal Barrier Layer Capacitor (IBLC) effect.<sup>4,5</sup> The IBLC model is widely accepted and implies the presence of conducting parts (grains) surrounded by insulating regions (grain boundaries). On the other hand, the giant permittivities for CCTO single crystals and/or thin films, where no grain boundaries are present, have been also explained by alternative mechanism such as non-ohmic contact between surface and electrode (Surface-Barrier-Layer-Capacitor SBLC effect).<sup>13–15</sup>

However, the giant permittivity phenomenon has been mainly studied and investigated on CCTO ceramics and the IBLC model

has been initially proposed on the basis of Impedance Spectroscopy results.<sup>4,5</sup> Nevertheless, interpretation of the physical properties of CCTO could certainly be improved by an investigation on the nanometre scale. In fact, several techniques based on Scanning Probe Microscopy (SPM) with conductive tips are useful for such investigation because they generally focus on information about the homogeneity of the sample. In this context, Kelvin Probe Force Microscopy studies on CCTO,<sup>12</sup> reinforced the possibility to explain the giant  $k$  phenomenon by the IBLC model.

On the other hand, a more recent report based on Conductive Atomic Force Microscopy (C-AFM) measurements of CCTO ceramics claims the presence of conducting grain boundaries, thus proposing the presence of a “percolation conducting network at the grain boundaries plus intragrain insulating interfaces”.<sup>16</sup> This interpretation has been challenged by other researchers.<sup>17,19</sup>

In the present paper, the dielectric behaviour of CCTO ceramics has been studied by C-AFM. The discrepancies among several earlier papers<sup>16–19</sup> have been discussed in terms of superficial artefacts affecting the SPM techniques, both from geometrical and electrical considerations. Dedicated methodologies on SPM techniques and sample section surface preparation have been improved to ensure robust and reliable investigation methods, especially working on heterogeneous materials such as CCTO.

In particular, we compare our results to earlier SPM investigations and provide insights towards the controversial

<sup>a</sup>Istituto per la Microelettronica e Microsistemi (IMM), Consiglio Nazionale delle Ricerche (CNR), Strada VIII 5, 95121 Catania, Italy. E-mail: raffaella.lonigro@imm.cnr.it; Fax: +39 095 5968312; Tel: +39 095 5968218

<sup>b</sup>Department of Materials Science and Engineering, University of Sheffield, Sir Robert Hadfield Building, Mappin Street, S1 3JD, Sheffield, UK

interpretation of existing literature data,<sup>16–19</sup> merging all of the reported conclusions on the physical nature of the grain boundaries and finally providing the ultimate C-AFM resolution and sensitivity for these heterogeneous materials.

## Results and discussion

### C-AFM analysis of $\text{CaCu}_3\text{Ti}_4\text{O}_{12}$ (CCTO) ceramics

The chemical and electrical nature of CCTO grain boundaries represents a much debated issue. The conducting<sup>16,18</sup> or insulating nature<sup>4,5,17,19</sup> of the CCTO grain boundaries has been the subject of a harsh debate which has included an animated discussion on the reliability and accuracy of the microscopic measurements. In this context, it should be noted that some data reported in previous literature papers<sup>16–19</sup> have been collected from samples prepared under different sintering conditions and it is well-known that the dielectric properties can be affected by the fabrication process. Thus, here, we propose an accurate study on CCTO ceramic pellets fabricated in the same conditions used in previous C-AFM works.<sup>16,18</sup>

The CCTO pellets, before and after the superficial polishing, have been characterized by X-Ray Diffraction (XRD), Scanning Electron Microscopy (SEM) and Energy Dispersive X-ray (EDX) analysis. Comparative studies have been performed on CCTO ceramics before and after the superficial treatments needed for the C-AFM investigation. In both cases they are polycrystalline (Fig. 1a) with grains more than 2  $\mu\text{m}$  wide (Fig. 1b and c) and their stoichiometry is almost ideal (1 : 2.87 : 3.98 Ca : Cu : Ti).

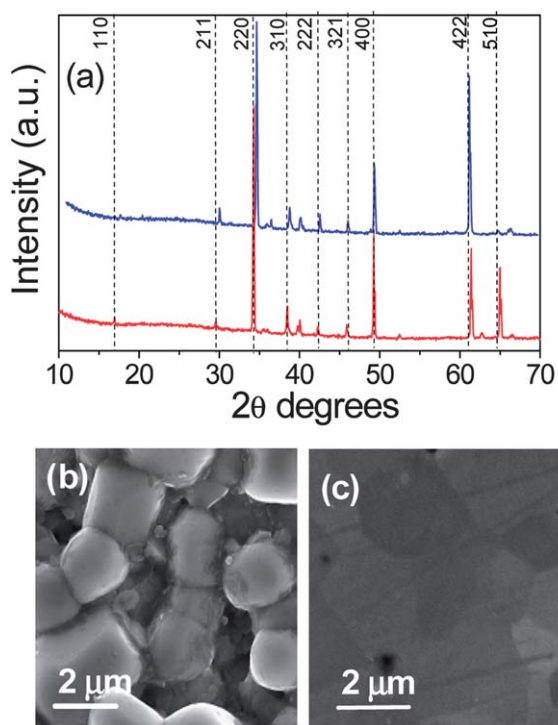


**Fig. 1** (a) XRD patterns of CCTO ceramics before (red line) and after (blue line) the superficial polishing and SEM images of CCTO ceramics before (b) and after (c) the superficial polishing.

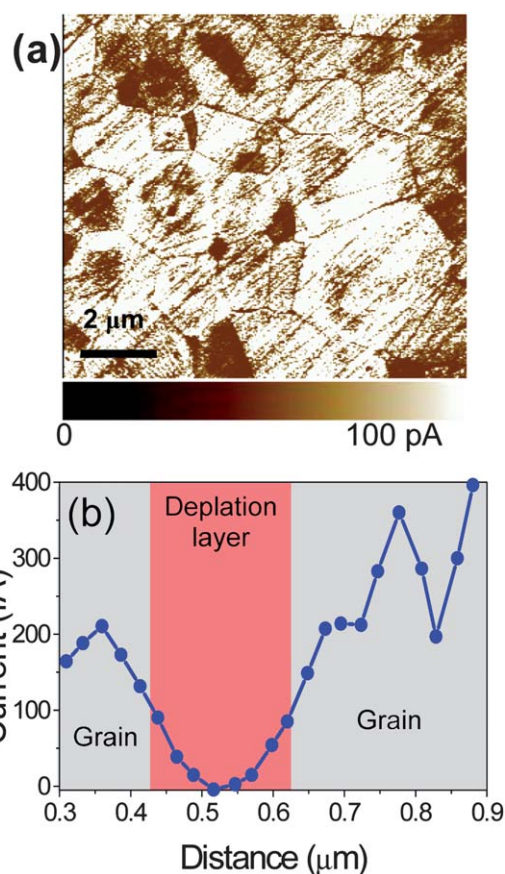


**Fig. 2** (a) Current map by C-AFM of CCTO ceramics and (b) current profile across the grain–grain boundary–grain structure.

In Fig. 2a the C-AFM current map acquired at 10 V is shown. The darker zones of the current map are associated with more insulating regions, which are located: (i) at the grain boundaries, (ii) some holes among three/four grains and (iii) at the center of few grains. The lower conductivity regions within some grains have been already discussed in an earlier publication<sup>20</sup> in terms of  $\text{CaTiO}_3$  inclusions within single grains. The current value at the grain boundaries is lower than in the grains even if some inclusions are present. The insulating layer thickness (depletion layer) at the grain boundaries is about 100 nm. This value has been evaluated by the full width at half maximum of the peak (see red part in Fig. 2b) visible in the current profile collected along the grain–grain boundary–grain region. This value is in good agreement with our previous Scanning Impedance Microscopy (SIM) investigation.<sup>20</sup>

The insulating region is wider than the physical grain boundary thickness (few nanometres) due to the presence of a potential barrier that produces a depletion of the semi-conducting (grains) materials.

In the literature, a specific C-AFM study on CCTO showed conducting grain boundaries, even though the SEM images indicated the samples were not well-polished.<sup>16</sup> On the other hand, a paper commenting on that C-AFM study claimed that the C-AFM technique is a deficient method to probe  $\sim\text{nm}$  grain boundaries because of its poor resolution.<sup>17</sup>

On the basis of these arguments, two main issues now need to be addressed:

- the criteria for reliable nano-electrical characterization, and
- the resolution limit for nano-electrical characterization.

Both issues, in turn, will now be discussed.

### SPM reliability

SPM techniques have been developed as important tools for the characterization of surface structures and chemical/physical properties in recent years.<sup>21</sup> SPM provides the possibility to investigate the electrical, topographic, magnetic and many other types of surface properties down to atomic resolution when physically allowed. Whatever the quality and mode of operation that Scanning Probe Microscopes are based on, the contact area must be kept constant. In the case of SPM applied to the study of electrical properties, the electrical quality of the contact should be validated. In particular, surface roughness and contamination can affect and even destroy the SPM electrical signal, thus the real case can be very far from the ideal one.

Flat surfaces favour enhanced lateral resolution even using commercial diamond polycrystalline tips, whose curvature radii are 20–50 nm. This supports the importance of the superficial low roughness requirement. The superficial roughness can be defined in several different ways. Numerous books are available reporting the image processing with matrices, Fourier analysis and statistical methods as autocovariance.<sup>21</sup>

The surface morphology has to be explained in terms of all the superficial components and each AFM image can be considered as the overlap of waves having circular symmetry and can be decomposed by Fast Fourier Transform (FFT). Features with different size and distribution can be present and the Root Mean Square (RMS) of an image height distribution is size ( $z$ ) dependent. The RMS increases upon increasing the scan size from zero up to the correlation length ( $L_c$ ), representing the limit for the saturation value to be achieved. This value is defined as the RMS intrinsic value. Moreover, surfaces with different features could possess the same RMS value but different peculiarities. Thus a more independent and confident parameter is the Power Spectral Density (PSD). The PSD( $f$ ), where  $f$  represents the roughness frequencies, is related to the FFT( $f$ ) and RMS by the following equations:

$$\text{PSD}(f) = |\text{FFT}(f)|^2 \quad (1)$$

and

$$\text{RMS}^2 = \sum_{k1}^{k2} \left| \text{FFT}(k) \right|^2 \quad (2)$$

The PSD( $f$ ) identifies the wave components contributing to the superficial topography. In particular, the PSD( $f$ ) components at lower frequency are related to the larger superficial features, while the high frequency PSD( $f$ ) components are associated with the smaller and flat superficial features. The exponential PSD decay vs.  $f$  indicates a roughness value comparable to an atomic flat surface.

In fact, an ideal polished surface is described by a Gaussian distribution of the measured surface heights ( $z(n)$ ) since the typical autocorrelation function for independent events is the Gaussian:

$$z(n) \propto \exp(-(z - \bar{z})^2/L_c^2) \quad (3)$$

with  $L_c$  being the correlation length and the PSD( $f$ ):

$$\text{PSD}(f) = \frac{2d_0}{N} \left| \sum_{n=1}^N e^{i2\pi(n-1)(m-1)} z(n) \right|^2 \quad \text{for } f = \frac{m-1}{Nd_0} \quad (4)$$

where  $i = \sqrt{-1}$ ,  $f$  = the frequency range from  $1/L$  to  $(N/2)/L$  and  $L$  is the digitized profile of length, consisting of  $N$  points sampled at intervals of  $d_0$  and  $m$  is an index related to the component involved in the FFT and it varies from 0 to  $N$ . It follows that the PSD( $f$ ) of an ideal polished surface should behave as a simple exponential decay vs.  $f$  (linear in a semi-logarithmic plot).

In the present work, the complete roughness investigation comes out from the PSD data versus frequency (Fig. 3a) measured on the CCTO surface. Initially, the surface treatment produces a strong roughness reduction eliminating the macroscopic sample defects such as hillocks and surface contamination. The saturation in the region of the lower PSD components (dashed circle in Fig. 3a) is already reached after the treatment with 1  $\mu\text{m}$  diamond paste, indicating that the larger features have been completely removed. The 1 and 0.1  $\mu\text{m}$  diamond paste treatments do not change the lower frequency contribution (already saturated, see the dash circle in Fig. 3a), but there is a strong PSD reduction at higher frequency (full circle). The exponential PSD decay vs.  $f$  after the 0.1  $\mu\text{m}$  diamond paste treatment indicates a roughness value comparable to an atomic flat sample in small (about  $10 \times 10 \mu\text{m}^2$ ) scanned regions

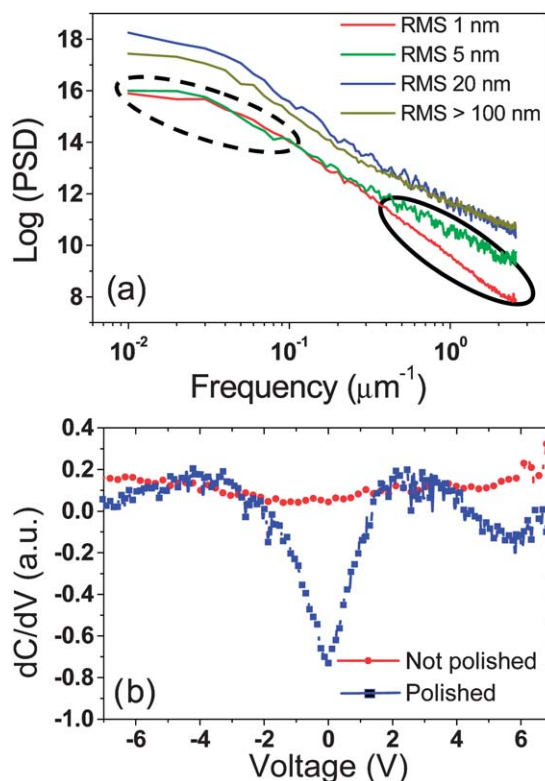


**Fig. 3** (a) PSD of the topographic CCTO image versus frequency after different superficial treatments and (b)  $dC/dV$  versus voltage curves obtained by SCM on both polished (blue curve) and not polished (red curve) CCTO surfaces.

(RMS  $\approx$  1 nm in regions which do not include any voids due to ceramic porosity).

An ideal polished surface, with a very low roughness with respect to the tip radius (10 nm) excludes geometrical artefacts. However, a physical criterion to evaluate the quality of the electrical contact between the sample surface and the nanometre probe needs also to be considered. Here, we suggest monitoring the electrical contact quality (sensitivity) between the probe and the sample surface by checking the Scanning Capacitance Microscopy (SCM) response because this kind of measurement is more sensitive than that obtained directly by C-AFM.

Fig. 3b shows the  $dC/dV$  versus voltage curves acquired on both the polished (blue curve) and unpolished (red curve) CCTO surfaces. The electrical sensitivity, as well as the capacitance response, is strongly influenced by surface conditioning. In fact, the  $dC/dV$  curve before polishing is almost constant over the whole applied voltage range. This behaviour can be explained with the presence of mobile charges on the sample surface compensating the charge accumulated at the tip/sample interface. In an unpolished condition, a non-quantified amount of charge is present and the contact is degraded. On the other hand, after the polishing treatment the surface shows ideal contact behaviour as in the case of an ideal Metal–Insulator–Semiconductor device or an ideal Schottky contact (blue curve). The peak position is centred on 0 V and this corresponds to a low fixed charge concentration which normally produces the peak shift. The tip therefore “locally probes” the sample properties, *i.e.* if it is conductive (ohmic response), semi-insulating or insulating (Schottky response) without the influence of surface charges.

As a first conclusion, we can safely confirm that C-AFM investigations on CCTO ceramics are reliable providing the PSD analysis of the surface and the sensitivity evaluation by SCM measurements are performed so as to exclude geometrical and electrical artefacts.

### C-AFM spatial resolution

It is well-known that during the commonly used fabrication process for perovskite oxides, a substantial increase in the point defect concentration (including ionic vacancies and free charge carriers) may be produced near the surfaces of each grain, resulting in modification of the dielectric properties. Here we have shown the imaging of such a grain–grain boundary (about 100 nm wide) dielectric structure by accurate C-AFM measurements. However, some authors<sup>17</sup> have claimed C-AFM does not have sufficient resolution to investigate grain boundaries.

Here, we determine the C-AFM resolution by investigation of an *ad hoc* fabricated sample. It consists of a 10 nm thermally grown silicon oxide layer on an n-type silicon wafer and on its top a 300 nm thick strongly doped polysilicon layer.

Fig. 4a shows the C-AFM map of the cross-section for the sample which was polished as described previously.

The insulating region corresponding to the SiO<sub>2</sub> layer is clearly visible as being sandwiched between the two conducting layers. During the C-AFM tip scanning there are three possible configurations identified in Fig. 4b by three different colours: grey, green and red. The grey portions correspond to the tip moving on the conducting polysilicon or silicon substrate. In

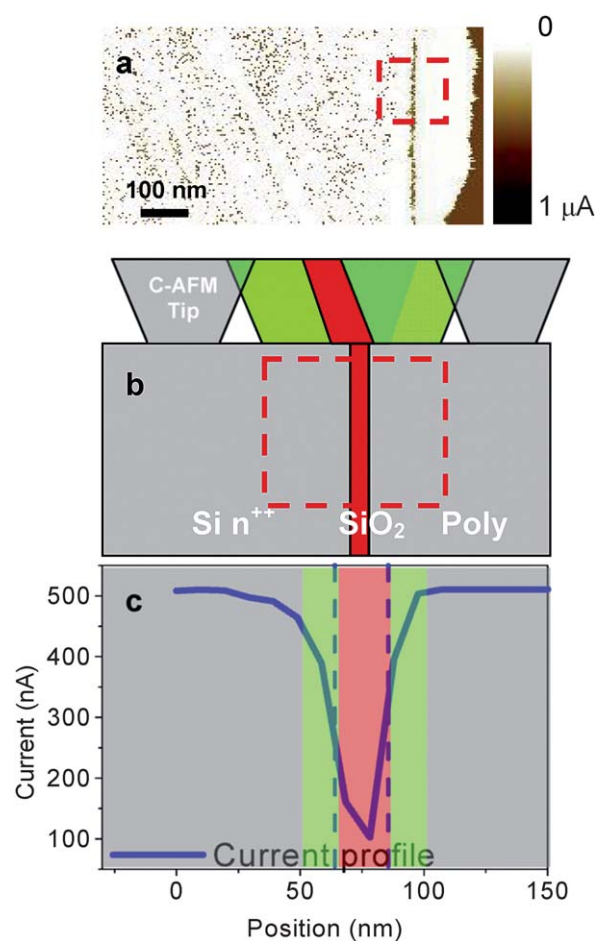


**Fig. 4** (a) C-AFM on the test sample (Si/SiO<sub>2</sub>/polySi) cross-section. Three different tip–sample configurations (b) and the current profile (c) across the sample.

these regions the current is at the highest level (blue line in grey parts in Fig. 4c). The green portions represent the tip partially overlapping the insulating SiO<sub>2</sub> layer (Fig. 4b) and the current value decreases in the profile (blue line in green parts in Fig. 4c). The red portion is related to the tip completely covering the insulating SiO<sub>2</sub> layer (Fig. 4b) and the current reaches the minimum value (blue line in red part in Fig. 4c).

The current profile (Fig. 4c) provides an estimation of our C-AFM resolution. In fact, the C-AFM resolution can be obtained by considering the full width at the half maximum of the peak in the current profile: it is 25 nm. The insulating region from the results is larger than the real SiO<sub>2</sub> thickness due to the tip size and effective contact area. Thus, with a tip radius 50 nm wide, the diameter of the contact area is 25 nm.

This result demonstrates that the estimated depletion layer at the grain boundaries for the CCTO ceramics is not overestimated because it is larger than the resolution limit, but instead it represents a realistic value.

In this context, it should be noted that the physical thickness of the grain boundaries (generally a few nm) should not be confused with the depletion layer thickness at the grain–grain boundary–grain interfaces. These depletion regions often protrude into the grains and originate from the presence of ionic vacancies, free charge carriers and/or compositional gradients on the outer

surfaces of the grains. Their development depends on the defect chemistry of the material under investigation and the processing conditions employed to prepare the samples.

Careful preparation and characterisation of sample surfaces to avoid artefacts and/or errors due to tip-sample interactions ensure that realistic quantification of electrically distinct layers having a thickness of few tens of nanometres can be achieved.

## Conclusion

Dielectric investigations on the nanometre scale by C-AFM measurements require a reliable and reproducible characterisation methodology. Here, two criteria have been proposed to carefully control the influence of the superficial features on the roughness (monitoring the PSD data of the surface roughness) and to provide an ideal electric contact between the probe and the sample surface (checking the  $dC/dV$  curve behaviour at the nanometre scale by SCM). In CCTO ceramics, semiconducting grains surrounded by insulating regions at the grain boundaries have been observed and because of the evaluation of possible artefacts, the detailed electrical structure at the grain boundaries has been imaged. These results demonstrate the validity of the IBLC effect to explain the macroscopic dielectric properties of CCTO ceramics.

## Experimental

### Fabrication of the $\text{CaCu}_3\text{Ti}_4\text{O}_{12}$ ceramics

$\text{CaCu}_3\text{Ti}_4\text{O}_{12}$  ceramics have been fabricated by a mixed oxide route already described in previous papers, and have been sintered at  $1050^\circ\text{C}$ .<sup>4,5</sup>

### Preparation of $\text{CaCu}_3\text{Ti}_4\text{O}_{12}$ ceramics for C-AFM measurements

The ceramic pellets (cut from the original discs) were polished to eliminate the influence of superficial artefacts in the tip contact when mapping by C-AFM. The surface of the CCTO pellets was smoothed by mechanical polishing using diamond pastes, with progressively thinner grid diameters, from 30 to  $1\ \mu\text{m}$ . The final polish was performed with a  $0.1\ \mu\text{m}$  diamond paste on a frosted glass plate. The final roughness (root mean square) value of the CCTO surface was  $\sim 1\ \text{nm}$  (excluding the contribution of voids due to porosity in the ceramics).

### C-AFM characterization

Power Spectral Density (PSD) analyses have been performed on AFM images acquired in non-contact (tapping) mode with silicon tips (curvature radius  $\approx 10\ \text{nm}$ ).

Electrical measurements at the nanometre spatial dimension were carried out by a Digital Instrument D3100 atomic force microscope equipped with a hybrid head and a Nanoscope V controller operating in air and in dark lift mode with diamond

tips (curvature radius  $\approx 50\ \text{nm}$ ). The measurements were performed using a back side contact, obtained by silver paint, opposite to the polished surface.

The quality of the electrical contact has been proved using Scanning Capacitance Microscopy (SCM). SCM measurements were carried out in constant  $\Delta V$  mode. The ac bias applied between the tip and sample was varied in the 1–10 V peak-to-peak range at 90 kHz with the resonator frequency  $1.0 \pm 0.1\ \text{GHz}$ .<sup>22</sup>

## Acknowledgements

This work has been supported by European Union under the project NUOTO (New Materials with Ultrahigh  $k$  dielectric constant for Tomorrow wireless electronics). NMP3-CT-2006-032644 and the Engineering and Physical Sciences Research Council (EPSRC).

## References

- 1 P. Lunkenheimer, S. Krohns, S. Riegg, S. G. Ebbinghaus, A. Reller and A. Loidl, *Eur. Phys. J. Spec. Top.*, 2010, **180**, 61.
- 2 M. A. Subramanian, D. Li, N. Duan, B. A. Reisner and A. W. Sleight, *J. Solid State Chem.*, 2000, **151**, 323.
- 3 C. Homes, T. Vogt, S. M. Shapiro, S. Wakimoto and A. P. Ramirez, *Science*, 2001, **293**, 673.
- 4 D. C. Sinclair, T. B. Adams, F. D. Morrison and A. R. West, *Appl. Phys. Lett.*, 2002, **80**, 2153.
- 5 T. B. Adams, D. C. Sinclair and A. R. West, *Adv. Mater.*, 2002, **14**, 1321.
- 6 W. Li and R. W. Schwartz, *Appl. Phys. Lett.*, 2006, **89**, 242906.
- 7 M. H. Cohen, J. B. Neaton, L. He and D. Vanderbilt, *J. Appl. Phys.*, 2003, **94**, 3299.
- 8 J. Li, M. A. Subramanian, H. D. Rosenfeld, C. Y. Jones, B. H. Toby and A. W. Sleight, *Chem. Mater.*, 2006, **16**, 5223.
- 9 R. Lo Nigro, R. G. Toro, G. Malandrino, M. Bettinelli, A. Speghini and I. L. Fragalà, *Adv. Mater.*, 2004, **16**, 891.
- 10 R. Lo Nigro, R. G. Toro, G. Malandrino, I. L. Fragalà, M. Losurdo, M. M. Giangregorio, G. Bruno, V. Raineri and P. Fiorenza, *J. Phys. Chem. B*, 2006, **110**, 17460.
- 11 G. Deng, T. Yamada and P. Muralt, *Appl. Phys. Lett.*, 2007, **91**, 202903.
- 12 S.-Y. Chung, I.-D. Kim and S.-J. L. Kang, *Nat. Mater.*, 2004, **3**, 774.
- 13 S. Krohns, P. Lunkenheimer, S. G. Ebbinghaus and A. Loidl, *Appl. Phys. Lett.*, 2007, **91**, 022910.
- 14 M. Li, Z. Shen, M. Nygren, A. Feteira, D. C. Sinclair and A. West, *J. Appl. Phys.*, 2009, **106**, 104106.
- 15 P. Fiorenza, R. Lo Nigro, V. Raineri, G. Malandrino, R. G. Toro and M. R. Catalano, *J. Appl. Phys.*, 2010, **108**, 074103.
- 16 D. Fu, H. Taniguchi, T. Taniyama, M. Itoh and S. Koshihara, *Chem. Mater.*, 2008, **20**, 1694.
- 17 S. Y. Chung, *Chem. Mater.*, 2008, **20**, 6284.
- 18 D. Fu, H. Taniguchi, T. Taniyama, M. Itoh and S. Koshihara, *Chem. Mater.*, 2008, **20**, 6286.
- 19 M. C. Ferrarelli, D. C. Sinclair, A. R. West, H. A. Dabkowska, A. Dabkowski and G. M. Luke, *J. Mater. Chem.*, 2009, **19**, 5916.
- 20 P. Fiorenza, R. Lo Nigro, C. Bongiorno, V. Raineri, M. C. Ferrarelli, D. C. Sinclair and A. R. West, *Appl. Phys. Lett.*, 2008, **92**, 182907.
- 21 Applied Scanning Probe Methods X, *Nanoscience and Technology series*, ed. B. Bhushan, H. Fuchs and M. Tomitori, Springer-Verlag, Heidelberg, 2008, ISBN: 978-3-540-74085-8.
- 22 P. Fiorenza, R. Lo Nigro, V. Raineri, S. Lombardo, R. G. Toro, G. Malandrino and I. L. Fragalà, *J. Appl. Phys.*, 2005, **98**, 044312.